Pharmaceutical Research, Vol. 23, No. 5, May 2006 (© 2006)
DOI: 10.1007/s11095-006-9901-9

Research Paper

Efficacy of siRNA Nanocapsules Targeted Against the *EWS–Fli1* Oncogene in Ewing Sarcoma

Nedjma Toub,[1,2] Jean-Rémi Bertrand,[2] Ali Tamaddon,[2] Hind Elhamess,[2] Hervé Hillaireau,[1] Andrei Maksimenko,[2] Jean Maccario,[3] Claude Malvy,[2,4] Elias Fattal,[1] and Patrick Couvreur[1]

Received August 29, 2005; accepted January 6, 2006

Abstract. The *EWS–Fli1* fusion gene encodes for a chimeric oncogenic transcription factor considered to be the cause of the Ewing sarcoma. The efficiency of small interfering RNAs (siRNAs) targeted toward the EWS–Fli1 transcript (at the junction point type 1) was studied, free or encapsulated into recently developed polyisobutylcyanoacrylate aqueous core nanocapsules. Because this mRNA sequence is only present in cancer cells, it therefore constituted a relevant target. Studies of the intracellular penetration by confocal microscopy in NIH/3T3 EWS–Fli1 cells showed that nanocapsules improved the intracellular penetration of siRNA with mainly a cytoplasmic localization. These biodegradable siRNA-loaded nanocapsules were then tested *in vivo* on a mice xenografted EWS–Fli1-expressing tumor; they were found to trigger a dose-dependant inhibition of tumor growth after intratumoral injection. A specific inhibition of EWS–Fli1 was observed, too. These findings now open new prospects for the treatment of experimental cancers with junction oncogenes.

KEY WORDS: Ewing sarcoma; EWS–Fli1; isobutylcyanoacrylate; nanocapsules; siRNA.

INTRODUCTION

Chromosomal translocations are found in special types of hematopoietic malignancies and sarcomas (1,2). Ewing sarcoma is a metastatic bone cancer of children and young adults. At the cellular level, poorly differentiated round cells characterize it; a genetic abnormality is associated with this malignancy, which consists in a rearrangement of chromosomes 22 and 11. The *EWS–Fli1* fusion gene, a product of the translocation t(11;22) (q24;q12), is detected in 90% of Ewing sarcomas and primitive neuroectodermal tumors (PNETs) (3). The *EWS–Fli1* results in the fusion of the carboxyl-terminal region of *Fli1* with the amino-terminal region of a putative RNA-binding protein, *EWS* (4,5). The chimeric EWS–Fli1 protein is believed to function as a transcriptional activator (4–8). The crucial role of this fusion protein in cellular proliferation has been demonstrated previously in Ewing sarcoma and PNET cells by using an antisense oligodeoxyribonucleotide as well as a small interfering RNA (siRNA), both targeted toward the *EWS–Fli1* (9,10). Thus, siRNA with relevant sequences may be considered for the treatment of cancers characterized by a fusion oncogene.

RNA interference (RNAi) is a process of sequence-specific, posttranscriptional gene silencing found in a variety of eukaryotes ranging from fungi to mammals (11–15). The mechanism of the target inhibition has been proposed to take place via 21–23 nucleotide siRNAs. Then, the siRNAs associate with a complex of proteins termed the RNA-induced silencing complex (RISC), which directs the siRNA to the complementary target sequence, resulting in the cleavage of the target RNA (15). The most potent siRNA duplexes are 19–21 nucleotides long, with two-nucleotide, 3′-overhanging termini (14). One strategy for the introduction of siRNAs into cells is their direct expression after intracellular expression of a small hairpin RNA (shRNA). An RNA polymerase III (pol III) transcription system produces an shRNA into the cell, which is then transformed in an active siRNA (16). Another method is to introduce the synthetic relevant siRNA sequence directly into the cells. However, in that case, the biological efficacy is hampered by the poor stability of siRNA in biological fluids and by their low intracellular penetration (17,18). Thus, nanocarrier systems, mainly cationic lipids, represent an option to improve the *in vivo* intracellular delivery of these nucleic acid-based drugs by protecting them from the harsh environment of the extracellular fluids (19–21). However, an important issue is that the cationic nature of these lipids leads to aggregation when administered systemically *in vivo*. This is the reason why, in this study, we have chosen to use noncationic polyisobutylcyanoacrylate nanocapsules with an aqueous core (22) for the delivery of siRNA targeted toward the *EWS–Fli1*

[1] Laboratoire de Physicochimie, Pharmacotechnie et Biopharmacie, Faculté de Pharmacie, UMR CNRS 8612, 92286 Châtenay-Malabry, France.
[2] Laboratoire de Vecterologie et Transfert des Gènes, Institut Gustave Roussy, UMR CNRS 8121, 39, rue Camille Desmoulins, 94805 Villejuif Cedex, France.
[3] Centre d' Etudes Pharmaceutiques, 12 roe J.B. Clément, 92296 Chatenay-Malabry Cedex, France.
[4] To whom correspondence should be addressed. (e-mail: cmalvy@igr.fr)

fusion oncogene. This formulation has been shown (a) *in vitro* to penetrate intracellularly and (b) *in vivo* to inhibit tumor growth in an experimental Ewing sarcoma. It is, to our knowledge, the first time that an siRNA against a fusion oncogene is efficiently delivered by means of nanotechnologies.

MATERIALS AND METHODS

Nucleic Acids

The oligonucleotides were purchased from Eurogentec (Seraing, Belgium). The siRNA target sequence is designed at the junction between *EWS* and *Fli1* in the chimeric mRNA (nucleotides 822–842). This sequence is specific of the tumor cells because the chimeric RNA is not expressed in normal cells. siRNAs with the following sequences were used:

- siRNA antisense (siRNA-AS). Sense strand: 5′-r(GCUACGGGCAGCAGAACCC)d(TT)-3′; antisense strand: 5′-r(GGGUUCUGCUGCCCGUAGC)d(TG)-3′
- Control siRNA (siRNA-Ct). Sense strand: 5′-r(GCUGCG GACAGCAGAAGCC)d(TT)-3′; antisense strand: 5′-r(GGCUUGUGCUGUCCGCAGC)d(TG)-3′

The two 3′-overhanging bases are synthesized with a DNA chemistry to enhance the siRNA nuclease resistance as described by Tuschl (23). The sense and antisense strands were hybridized in 30 mM HEPES–KOH (pH 7.4), 2 mM Mg-acetate, 100 mM K-acetate for 1 min at 95°C (final volume 100 μl), and then for 1 h at 37°C to obtain a final stock concentration of 50 μM. siRNAs have been purified by high-performance liquid chromatography (HPLC) and then controlled by mass spectrometry (Eurogentec).

siRNA Radiolabeling

The 5′-end of one strand of the duplex was labeled by T4 polynucleotide kinase (New England Biolabs, Frankfurt am Main, Germany) with [γ-^{32}P]ATP (111 TBq/mmol; MP Biomedicals, Illkirch, France) under the conditions indicated by the manufacturers. The purified strands were recovered by gel filtration using a Bio-Spin 6 column (BioRad, Richmond, CA, USA) and centrifuged at 2500×*g* for 4 min. The purity was then controlled by radioactivity analysis using an automatic-TLC-linear analyzer (EG&G Berthold, Elancourt, France) as described by Aynie *et al.* (24).

Nanocapsule Preparation and siRNA Encapsulation

The preparation of an aqueous suspension of polyisobutylcyanoacrylate nanocapsules containing siRNA in their aqueous core was performed by modification of the method of Lambert *et al.* (25) and Watnasirichaikul *et al.* (26) as follows. We first prepared a nanoemulsion at 4°C by mixing 0.1 mL of demineralized water containing 0.5 mM (equivalent to 700 μg) siRNA duplex to an organic phase containing 1.125 g of Montane 80 (sorbitan monooleate, Seppic, Paris, France) and 1 g of Miglyol 812 (medium chain triglyceride, Sasol, Witten, Germany) using an Ultraturrax for 1 min at 24,000 rpm (4°C). Then, 10 mg of isobutylcyanoacrylate (IBCA) monomer (Loctite, Dublin, Ireland) was added rapidly to the nanoemulsion under mechanical stirring (500 rpm, room temperature). The system was left for at least 4 h for polymerization to take place. Nanocapsules were collected by ultracentrifugation at 30,000 rpm for 30 min at 4°C (Beckman L8-70M Ultracentrifuge, 50 Ti rotor). After liquid-phase removal, the pellet was transferred to a new tube and resuspended under vortex agitation (1 min) in sterile demineralized water (or physiological serum for animal experiments) at the desired siRNA concentration. The nanocapsule suspension was then dispersed by fast sonication (8 s) and centrifuged at 4000×*g* for 10 min (4°C) to remove residual surfactant. This process was repeated twice to insure complete nanocapsule purification.

Nanocapsule Characterization

The particle size and distribution of the nanocapsules was measured after dilution (1:30) in demineralized water using dynamic laser light scattering (Nanosizer ND4, Coultronics, Margency, France). The zeta potential of nanocapsules was determined as follows: 200 μl of the samples was diluted in 2 mL of a 0.1 mM KCl solution adjusted to pH 7.4 and analyzed with a Zetasizer (Malvern Instruments, Malvern, UK).

siRNA nanocapsules were incubated for 1 month in phosphate-buffered saline (PBS). Then, after ultracentrifugation (60,000×*g* for 30 min), supernatants were analyzed by polyacrylamide gel electrophoresis (PAGE; 20%) for siRNA integrity.

Freeze Fracture Electron Microscopy

A small drop of the suspension containing 30% of glycerol as cryoprotectant was deposited on a thin copper plate and rapidly frozen in liquid propane. Fracturing and replication (using Pt carbon) were performed with a Balzers BAF 301 freeze etch. The replicas were washed and examined under a Philips 410 electron microscope.

Determination of siRNA Encapsulation Yield

After [γ-^{32}P]ATP labeling, siRNAs were introduced into nanocapsules as described above. After the first ultracentrifugation, the radioactivity of supernatant and pellet was determined by the Cherenkov effect using a liquid scintillation counter (1900TR Packard). The final encapsulation yield was calculated as the ratio of the pellet radioactivity to the total used radioactivity (pellet + supernatant).

Cell Penetration Studies

NIH/3T3 cells stably transfected with the human *EWS–Fli1* gene were a generous gift from Dr. J. Ghysdael (Institut Curie, Orsay, France). We followed the intracellular trafficking of the siRNA by confocal microscopy using a rhodamine-labeled siRNA. Briefly, 10^5 NIH/3T3 EWS–Fli1 cells were seeded into six-well plates containing a cover glass in 1 mL of Dulbecco's modified Eagle's medium (DMEM; Gibco, Karlsruhe, Germany) supplemented by 10% heat-inactivated newborn calf serum (Gibco), penicillin, and streptomycin. The cells were then incubated overnight at

37°C with 5% CO_2 in a moist atmosphere. The medium was discarded, and a fresh one containing 25 nM (equivalent to 350 ng) of rhodamine-labeled siRNA free or encapsulated into nanocapsules, was added for 1, 2, and 4 h of incubation. The cells were then washed with PBS and fixed in PBS containing 2% paraformaldehyde for 20 min at room temperature. The slides were then observed with a confocal microscope (Zeiss LSM 510/Axiovert 200M with a 63×/1.4 oil immersion objective) after Mowiol (Calbiochem, Bad Soden, Germany) mounting as an antifading agent.

In Vitro Cell Treatment with Vectorized siRNA

NIH/3T3 or NIH/3T3 EWS–Fli1 cells were seeded onto six-well plate at 2×10^5 cells/well 1 day before the treatment in 1 mL of DMEM (Invitrogen, Carlsbad, CA, USA) containing 10% heat-inactivated newborn calf serum (Invitrogen) and penicillin–streptomycin (Invitrogen). Then, the medium was replaced by 900 µl of fresh medium and 100 µl of 100 mM NaCl, 10 mM HEPES, pH 7.2, containing 0.7 µg cytofectin (Gene Therapy Systems, San Diego, CA, USA) either free or complexed with 50 nM siRNA. Incubation was performed for 24 h at 37°C, 5% CO_2 in a moist atmosphere.

Cell survival was determined by the MTT test performed as follows. Cells were incubated for 2 h after adding 100 µl of a 5 mg/mL MTT (Sigma, Saint Quentin Fallavier, France) solution in PBS. Then, the cells were lysed by 1 mL of a 10% sodium dodecyl sulfate (SDS), 10 mM HCl solution overnight. The produced formazan was solubilized and quantified by an OD determination at 570 nm. Results are expressed as a percentage of untreated cells.

For the determination of the EWS–Fli1 expression, treated cells were lysed with 400 µl of 4 M guanidium thiocyanate, 25 mM Na-citrate (pH 7), 0.5% sarcosyl, and 0.1 M β-mercaptoethanol. Total RNA was then extracted after addition of 40 µl of 2 M Na-acetate (pH 4), 400 µl of water-saturated phenol, and 120 µl of chloroform/isoamyl alcohol (49:1). Three hundred microliters of the aqueous phase was precipitated with 300 µl of isopropanol. After centrifugation at 13,000 rpm for 15 min, the pellet was washed with 180 µl of 70% ethanol, air-dried, and dissolved in 10 µl of water containing 5 U RNasin (Promega, Madison, WI, USA). The RNA concentration was determined by spectrophotometry at 260 nm.

siRNA Administration to the Nude Mice

Murine fibroblasts NIH/3T3 stably transfected with the human *EWS–Fli1* fusion gene were harvested from 60% confluent monolayer cultures and resuspended in sterile 9 g/l NaCl at 2×10^7 cells/mL, and 100 µl of the suspension was subcutaneously inoculated into irradiated athymic nude mice. The tumor appeared in around 2 weeks, and the mice were then treated by intratumoral injection (in the tumor, horizontally, using a Microlance 30-gauge needle, mice being anesthetized by gaseous isoflurane) of 100 µl of siRNA free or encapsulated at a concentration of 1.6 µM (equivalent to 88 µg/kg in 9 g/l NaCl). The saline solution alone was used for control mice. Two distinct protocols were used (protocols are summarized in Table I).

In the first protocol, the animals received a dose of 40 µg of polymer in each injection. The complete treatment (nine injections) corresponded to a cumulative dose of 0.8 mg/kg (1.44 nmol) of siRNA and 360 µg of polymer for siRNA-AS, siRNA-Ct, siRNA-AS nanocapsules (NC siRNA-AS), and siRNA-Ct nanocapsules (NC siRNA-Ct). The nine injections were made at days 1, 2, 3, 6, 8, 10, 13, 15, and 17.

Table I. Different Treatment Conditions for siRNA Administration to Xenografted EWS–Fli1 Mice (Two Protocols: Cumulative Doses of 0.8 and 1.1 mg/kg)

	Single injection		Cumulative dose	
	siRNA (µg)	Polymer (µg)	siRNA (mg)	Polymer (µg)
First treatment protocol				
NC siRNA-AS	88	40	0.8	360
NC siRNA-Ct	88	40	0.8	360
siRNA-AS	88	0	0.8	0
siRNA-Ct	88	0	0.8	0
Control	0	0	0	0
Second treatment protocol				
NC siRNA-AS	220	40	1.11	200
NC siRNA-Ct	220	40	1.11	200
siRNA-AS	220	0	1.11	0
siRNA-Ct	220	0	1.11	0
Control	0	0	0	0

In the second protocol, the mice received a dose of 40 µg of polymer in each injection. The complete treatment (five injections) corresponded to a cumulative dose of 1.1 mg/kg (2 nmol) of siRNA and 360 µg of polymer for NC siRNA-AS, NC siRNA-Ct, and empty nanocapsules. Five injections were made at days 1, 3, 6, 9, and 12.

The tumor volume was determined during the experiments by two perpendicular measurements of the length (a) and width (b) of the tumor and was calculated as $ab^2/2$. The tumor growth indicated during the treatment was evaluated relatively to the initial day of the treatment.

The experiments were carried out on five to six animals per point, and the error bars correspond to the standard deviation.

Animals were housed and handled according to the recommended guidelines (27). They were humanely sacrificed by CO_2 inhalation.

Statistical Analysis

The p values, obtained by analysis of covariance using the two-way ANOVA test (GraphPad Prism Version 4.01), are those of the comparisons of tumor size to saline-treated animals at all days (1, 3, 6, 9, 12, and 15), using size at day 1 as covariable and treatments as factors. Tests were considered significant when the p values were less than 0.05.

RNA Extraction from Tumors

RNA extraction from the tumor was performed with a TRIzol® solution (Invitrogen) according to the manufacturer's instructions. Briefly, 100 mg of frozen tissue was added to a tube containing 1 mL TRIzol®, homogenized with a FastPrep system (Qbiogene, Illkirch, France) for 30 s and then centrifuged at 14,000 rpm for 5 min at 4°C. A 200-µl chloroform solution was added to 800 µl supernatant, vortexed, and

centrifuged at 14,000 rpm for 15 min. The total RNA present in the aqueous phase (300 µl) was precipitated by 300 µl isopropanol for 1 h at −20°C and centrifuged at 14,000 rpm for 15 min at 4°C. The pellet was washed with 70% ethanol, dried, and reconstituted in 10 µl of RNasin 1 U/µl (Promega). RNA concentration and purity were determined by spectrophotometry (28).

EWS–Fli1 and *EWS* Detection by Reverse Transcription-Polymerase Chain Reaction

The RNA quality was evaluated by 1% agarose gel electrophoresis followed by ethidium bromide staining. Then, 1 µg of total RNA was reverse-transcribed with random hexamers using M-MLV first-strand kit (Promega) according to the manufacturer's instructions. PCR amplification was performed in a final volume of 50 µl, containing 5 µl PCR buffer 10×, 200 µM dNTP, 35 pmol of each primer, and 2.5 U Taq DNA Polymerase (New England Biolabs). Two sets of primers were used to study both *EWS* (forward 5′-AGC AGT TAC TCT CAG CAG AAC ACC-3′, reverse 5′-TCC ACC AGG CTT ATT GAA GCC ACC-3′) and *EWS–Fli1* (forward 5′-AGC AGT TAC TCT CAG CAG AAC ACC-3′, reverse 5′-CCA GGA TCT GAT ACG GAT CTG GCT G-3′) gene expressions. The amplification profile was as follows: denaturation at 94°C for 30 s, primer annealing at 61°C for *EWS–Fli1* and 63°C for *EWS* for 30 s, and extension at 74°C for 1 min, for a total of 35 cycles in a PCR thermal cycler (MJ Research, Watertown, MA, USA**)**. To confirm that an equal amount of RNA was reverse-transcribed to cDNA, PCR amplification was run for the housekeeping gene *GAPDH* (forward 5′-GAC AAC TCA CTC AAG ATT GTC AG-3′, reverse 5′-CAT TGT CAT ACC AGG AAA TG-3′). Five-microliter PCR reaction of all three genes was loaded onto 1% agarose gel in Tris–acetate–EDTA (TAE) buffer, and amplified segments were detected by ethidium bromide staining. Data were analyzed using UN-SCAN-IT software.

RESULTS

Nanocapsule Characterization

After siRNA encapsulation, physicochemical characteristics of the produced particles and encapsulation yield were determined. The mean diameter of the nanocapsules, as measured by laser light scattering through unimodal analysis, was 325 nm, with a polydispersity index of 0.1 [number of measurements (n) = 10]. These results were confirmed by electronic microscopy showing circular regular particles with a size of 300 nm, as illustrated in Fig. 1. The thin polymer membrane forming the shell of the capsule is clearly observable on these pictures.

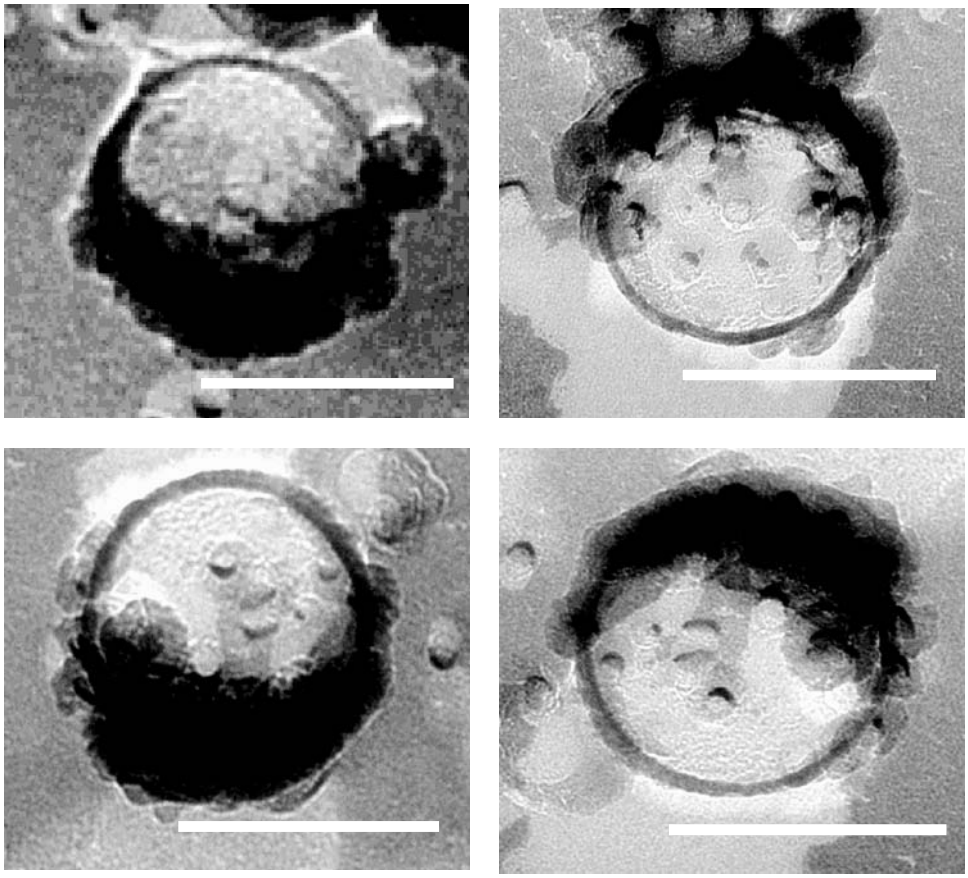

Fig. 1. Visualization by electron microscopy after freeze fracture of siRNA-loaded nanocapsules. The scale bar was 300 nm. The technique of freeze fracture electron microscopy requires a high dilution of the nanocapsules; thus, only few are seen on each grid and far apart from each other.

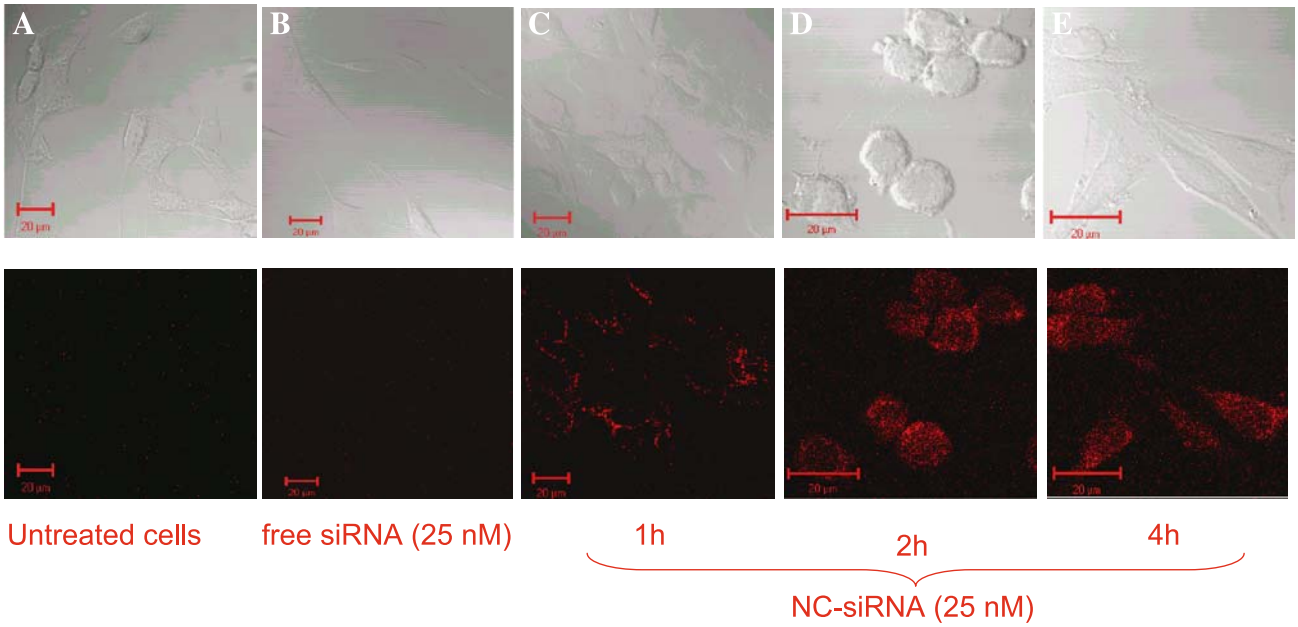

Fig. 2. Confocal microscopy of NIH/3T3 EWS–Fli1 cells after 1-h incubation of untreated cells (A), cells treated with free rhodamine-labeled siRNA free (B), and rhodamine-labeled siRNA nanocapsules for 1 h (C), 2 h (D), and 4 h (E). The concentration of rhodamine-labeled siRNA was 25 nM, and for the nanocapsule samples, polymer concentration was 100 μg/mL. Top: phase contrast image; bottom: fluorescence detection.

The yield of siRNA encapsulation was determined as 97.8 ± 0.5% through the use of ^{32}P-labeled siRNA (see "Materials and Methods"). After being released and tested by PAGE, the siRNA was found to comigrate with the initial siRNA before encapsulation and did not display any band broadening (data not shown).

The nanocapsules were found to be negatively charged, with a mean zeta potential value of −28 mV. This value was not modified after siRNA encapsulation, which is consistent with the fact that these molecules were efficiently encapsulated and not adsorbed at the nanocapsule's surface.

Intracellular Localization and Activity of siRNA

To determine whether nanocapsules were able to deliver siRNA into tumor cells, the intracellular distribution of the rhodamine-labeled siRNA was investigated by laser confocal microscopy after incubation of siRNA (free or encapsulated) with NIH/3T3 cells expressing EWS–Fli1 (Fig. 2).

Confocal microscopic analysis showed that the intracellular fate of encapsulated and free siRNA was dramatically different. Whereas free siRNA added to the culture media produced a low fluorescence localized on the extracellular matrix (Fig. 2B), bright punctuated rhodamine fluorescence was observed with the cells treated with siRNA nanocapsules (Fig. 2C–E). This red color was located intracellularly into the cell cytoplasm and as punctuate vesicles, suggesting a likely endosomal localization of the siRNA nanocapsules. This distribution and the time-dependent enhancement of the intracellular signal of fluorescence suggested an endocytic pathway for the nanocapsule uptake for 1–4 h of incubation.

Concerning cell growth inhibition, no activity was observed until a concentration of 50 nM, neither with free siRNA nor with siRNA in nanocapsules, whereas the siRNA sequence was found to decrease the EWS Fli-1 mRNA level after normalization by G3PDH (60% inhibition after 24 h and no inhibition with the control siRNA) (Fig. 3). For higher concentration, the cytotoxicity caused by the polymer was observed as tested with empty nanocapsules.

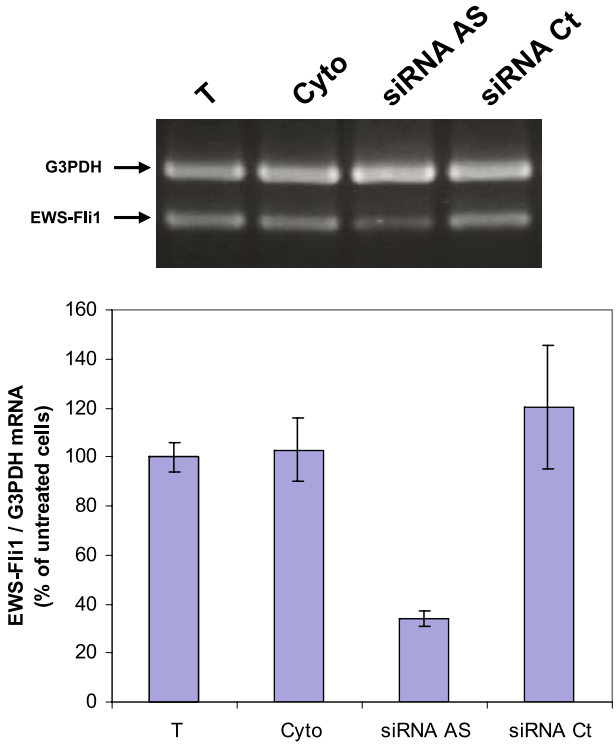

Fig. 3. Reverse transcription-polymerase chain reaction (RT-PCR) measurement shows that 50 nM siRNA transfected with cytofectin inhibits EWS–Fli1 expression in NIH/3T3 EWS–Fli1 cells after 24 h. Experiments were performed in triplicate.

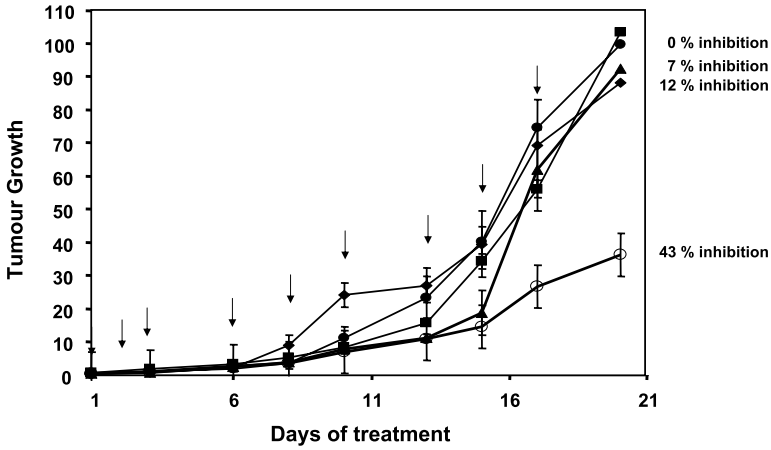

Fig. 4. Inhibition of EWS–Fli1-expressing tumor growth in nude mice by siRNA nanocapsules at a dose of 0.8 mg/kg. The treatment was performed by intratumoral administration for 20 days. Arrows correspond to the days of treatment. The effect of antisense siRNA in nanocapsules on tumor growth in nude mice is expressed relatively to tumor volume on day 1 according to the following formula: tumor volume at day *x*/tumor volume at day 1. Nine injections were performed at days 1, 2, 3, 6, 8, 10, 13, 15, and 17. All siRNA, free or encapsulated (NC), were used at a dose of 88 μg for each injection. The cumulative dose of siRNA was 0.8 mg/kg (1.44 nmol). ○, NC siRNA-AS; ▲, NC siRNA-Ct; ■, siRNA-AS; ♦, siRNA-Ct;●, saline. Bars indicate the standard deviation of the mean for six mice.

Administration to Mice

As explained in "Materials and methods," two different protocols were used for the intratumoral administration of siRNA to the EWS–Fli1 grafted mice. In the first therapeutic scheme and as shown in Fig. 4, only intratumoral injections of NC siRNA-AS led to a significant inhibition in the tumor growth at a cumulative dose of 0.8 mg/kg (1.44 nmol). This effect corresponded to a 3-fold decrease of tumor growth when compared with the control mice (0.9% NaCl). Under the same conditions, no effect could be detected after injection of the free siRNA.

In the second therapeutic scheme (1.1 mg/kg of cumulative dose, five injections), a still greater inhibition (80%) of tumor growth was obtained. However, unexpectedly, a stimulation of the tumor growth was observed with control

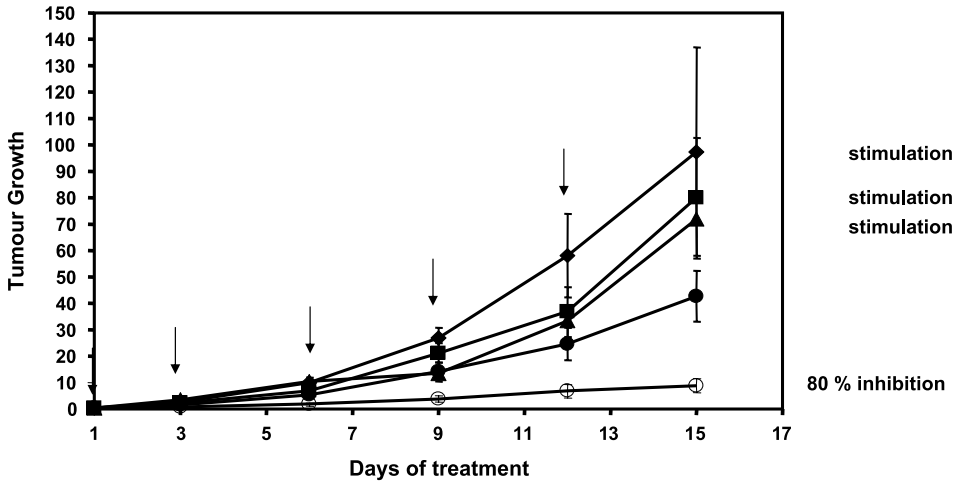

Fig. 5. Inhibition of EWS–Fli1-expressing tumor growth in nude mice by siRNA nanocapsules at a dose of 1.11 mg/kg. The treatment was performed by intratumoral administration until day 15. Arrows correspond to the days of treatment. The effect of antisense siRNA in nanocapsules on tumor growth in nude mice is expressed relatively to tumor volume on day 1 according to the following formula: tumor volume at day *x*/tumor volume at day 1. Five injections were performed at days 1, 3, 6, 9, and 12. All siRNA, free or encapsulated (NC), were used at a dose of 220 μg for each injection. The cumulative dose of siRNA was 1.11 mg/kg (2 nmol). ○, NC siRNA-AS; ▲, NC siRNA-Ct; ■, siRNA-AS; ♦, siRNA-Ct; ●, saline. Bars correspond to the standard deviation for six mice.

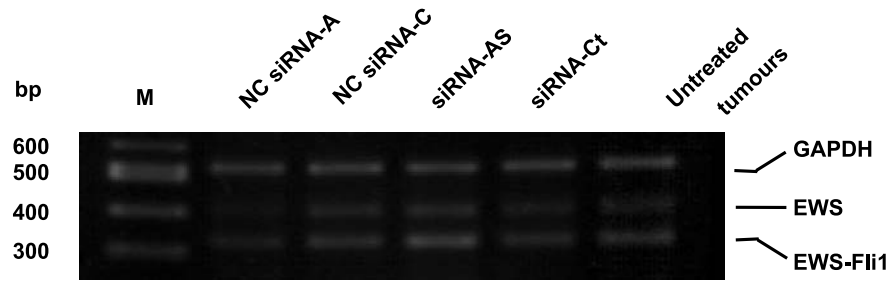

EWS-Fli1/GAPDH (% of untreated tumour)	57 ± 18	134 ± 32	274 ± 123	257 ± 139	100 ± 7
EWS/GAPDH (% of untreated tumour)	39 ± 7	106 ± 16	220 ± 96	222 ± 94	100 ± 12

EWS and EWS-FLI-1 gene expression is normalized by GAPDH expression and expressed as % of untreated mice (average of 3 independent experiments)

Fig. 6. RT-PCR measurement shows that siRNA nanocapsules inhibit *EWS–Fli1* and *EWS* expressions into mice grafted tumors.

siRNA administered either free or encapsulated (Fig. 5), whereas the same was observed with empty nanocapsules (data not shown).

The statistical analysis of covariance, with the tumor volume at day 1 as a covariable, showed that the NC siRNA-AS gave a significant inhibition when compared with saline-treated animals ($p < 0.0003$). The NC siRNA-Ct gave no inhibition ($p = 0.3544$). The free siRNA-AS and siRNA-Ct produced a nonsignificant stimulation of tumor growth. p values are 0.73 and 0.25, respectively (six animals in each group).

Tumor *EWS–Fli1* and *EWS* Expressions

For this purpose, we have developed a method to measure simultaneously the expressions of *EWS–Fli1* and *EWS*. Because in mice the *Fli1* gene was not expressed, it was important to measure the *EWS* status at the same time than the *EWS–Fli1* fusion gene to have a better appreciation concerning the specificity of the siRNA used. Thus, as explained in "Materials and methods," after total RNA extraction from the tumor, the expressions of *EWS–Fli1* (322 bp), *EWS* (396 bp), and the housekeeping gene *GAPDH* (531 bp) were monitored by reverse transcription-polymerase chain reaction (RT-PCR). As observed in Fig. 6, very little variation of *GAPDH* expression was observed in all the experimental points. This makes it possible to compare the expression of the target gene in the various slots after *GAPDH* normalization. Intratumoral injection of naked antisense and control siRNA resulted in a stimulation of both *EWS–Fli1* and *EWS* gene expressions. Application of nanocapsulated antisense siRNA decreased both *EWS–Fli1* and *EWS* gene expressions to 43 and 61%, respectively, as compared with the level measured in the nontreated tumors. There remained a stimulation of both gene expressions after application of control siRNA encapsulated into nanocapsules.

DISCUSSION

Inhibition of gene expression by short double-stranded RNA (siRNA) is a promising strategy to develop therapeutic applications. In animals, one of the limiting steps is a rapid RNA degradation and poor intracellular delivery. To overcome these limitations, particulate drug carriers may be used (29,30). In this study, we have employed the previously described polyisobutylcyanoacrylate nanocapsules (25) to deliver siRNA *in vivo* because these nanocapsules have been shown to be capable of protecting the encapsulated nucleic acid (i.e., oligonucleotide) toward nuclease degradation (25). It is noteworthy that, for this application, we have used a smaller preparation volume [2 mL instead of 4.5 mL in (22)], which has resulted in an extremely high encapsulation rate of siRNA of 97%, as compared with 81% of encapsulation yield with oligonucleotides (25). It is possible that the efficacy of stirring with an appropriate stem has led to a better dispersion of the water droplets in the oily nanoemulsion.

To determine the ability of such complexes to deliver efficiently the siRNA intracellularly, we have measured the *in vitro* cell penetration of rhodamine-labeled siRNA nanocapsules. By confocal microscopy, we observed (Fig. 2) that fluorescent siRNA was time-dependently captured by the cells with cytoplasmic and endosomal localizations (Fig. 2C–E). This effect was not observed after the cells were incubated with free siRNA (Fig. 2B). This significant fluorescent enhancement with nanocapsules revealed a high level of siRNA cell uptake and a clear punctuated perinuclear localization, which fits with a capture of the nanocapsules through an endocytotic pathway. However, using the MTT assay, no cell growth inhibition until an siRNA concentration of 50 nM was observed, which was therefore not caused by the inability of the siRNA nanocapsules to cross the cell membrane. It was neither caused by the inability of siRNA to inhibit its target mRNA because it was shown that using the same siRNA sequence, inhibition of EWS–Fli1 mRNA was efficiently obtained. This demonstrates again that cell culture experiments are not at all predictive of the *in vivo* data (see

below), even when they were performed on exactly the same tumoral cell line. We have already observed such a phenomenon with chitosan-coated nanospheres (35). The reasons of such a discrepancy are numerous and have already been discussed previously by others (36).

To evaluate the therapeutic efficacy of siRNA nanocapsules *in vivo*, we have tested the ability of this formulation to inhibit tumor growth in an Ewing sarcoma model. The animals were treated by intratumoral injection of either the siRNA free or encapsulated in two protocols: (a) one injection every 2 days, nine injections (0.8 mg/kg cumulative dose; 1.44 nmol); (b) one injection every 3 days, five injections (1.1 mg/kg cumulative dose; 2 nmol). The second protocol was proposed because it was expected that the encapsulated siRNA would be stable enough in cells after delivery, allowing to prolong the time between two injections. Additionally, such treatment was supposed to be better tolerated by the animals. For both treatments, a dramatic inhibition of tumor growth was observed but with a still greater effect in the second case (43 and 80%, respectively) (Figs. 4 and 5). For both protocols, the siRNAs alone had no inhibitory effect and even had a tendency to stimulate tumor growth. A similar stimulation of *EWS–Fli1* has already been observed previously in cell culture with free oligonucleotides (V. Pollard, personal communication). We suggest that this unspecific stimulation of NIH/3T3 EWS–Fli1 cells could be as a result of a nonspecific polyanionic effect of negatively charged molecules such as nucleic acids or nanocapsules. The hypothesis is that receptors for polyanions could be present on the outside of the cell membrane. When protected by the encapsulation, the siRNA could not induce such an unspecific effect, but the nanocapsules which are negatively charged (zeta potential of the surface was −28 mV) might play the same role (result not shown).

These data of tumor growth inhibition by siRNA nanocapsules resulted from a specific silencing inhibition of gene expression. By real-time RT-PCR on RNA extracted from treated tumor, a decrease of the *EWS–Fli1* RNA expression was indeed observed. According to the known mechanism of action of siRNAs, this should be due mainly to the RISC-dependent degradation of the targeted mRNA. Alongside this inhibition, an *EWS* inhibition was also observed, which is probably caused by the 17 bases of the siRNA also targeting the *EWS* gene. Owing to the literature, it is unlikely that the tumor inhibition is caused by *EWS* inhibition. It is, however, conceivable that some synergistic effect could take place when inhibiting both genes. It has indeed been shown that *EWS* and *EWS–Fli1* proteins form heterodimers (31).

It is now planned to test other siRNAs that would not inhibit *EWS* to closely investigate the role of *EWS* in the tumor inhibition that we have observed.

These results show the interest of nanocapsules for siRNA delivery *in vivo*. Many publications have described the potency of siRNAs for cellular gene inhibition [for a review, see (29,30,32)]. More recently, several reports have shown that protection of siRNAs by particulate vectors is a valuable approach for *in vivo* gene inhibition (33,34).

siRNA or antisense oligonucleotides will not be a substitute for cancer chemotherapy but an additive to it and to other therapies. This can take place either when there is a synergy between antisense compounds and other anticancer drugs or to maintain the residual disease at the background level with treatments which should be far less toxic than the usual cancer chemotherapy. Many recurrences happen after classical treatments because of micrometastases, which have escaped this treatment.

We demonstrate here that a potent activity can be obtained, as a result of nanoencapsulation, with an siRNA, which is targeted to a fusion gene considered to be the cause of the tumor.

A promising outcome of this research would be the possibility of treating Ewing sarcoma and PNET with various types of specific nucleic acids protected by polymeric encapsulation.

CONCLUSION

The present study reports for the first time the use of aqueous core nanocapsules for the delivery of siRNA to tumors with a junction oncogene as a specific target. Owing to the efficient intracellular penetration and to the *in vivo* anticancer activity, this type of formulation is promising for the treatment of cancers such as Ewing sarcoma and PNET.

ACKNOWLEDGMENTS

We thank Mr. Jalil Abdelali and Mrs. Monique Stanciu (G. Roussy Institute) for excellent technical assistance and Mrs. Ghislaine Frébourg (UMR CNRS 7138) for electronic microscopy experiments. N. Toub is supported by a fellowship from La Ligue Nationale Contre le Cancer. This work was supported by the Association de Recherche sur le Cancer (grant no. 4310), Fondation de l'Avenir, and the European grant PROTHETS (contract no. LSHC-CT-2004 5033036).

REFERENCES

1. T. H. Rabbitts. Chromosomal translocations in human cancer. *Nature (Lond.)* **372**:143–149 (1994).
2. C. Sreekantaiah, M. Ladanyi, E. Rodriguez, and R. S. K. Chaganti. Chromosomal aberration in soft tissue tumours. *Am. J. Pathol.* **144**:1121–1134 (1994).
3. O. Delattre, J. Zucman, B. Plougastel, C. Desmaze, T. Melot, M. Peter, H. Kovar, I. Joubert, P. D. Jong, G. Rouleau, A. Aurias, and G. Thomas. Gene fusion with an ETS DNA-binding domain caused by chromosome translocation in human tumors. *Nature (Lond.)* **359**:162–165 (1992).
4. T. Ohno, V. N. Rao, and E. S. Reddy. EWS/Fli1 chimeric protein is a transcriptional activator. *Cancer Res.* **53**:5859–5863 (1993).
5. R. A. Bailly, R. Bosselut, J. Zucman, F. Cornier, O. Delattre, M. Roussel, G. Thomas, and J. Ghysdael. DNA-binding and transcriptional activation of the EWS-FLI-1 fusion protein resulting from the t(11;22) translocation in Ewing sarcoma. *Mol. Cell. Biol.* **14**:3230–3241 (1994).
6. W. A. May, S. L. Lessnick, B. S. Braun, M. Klemsz, B. C. Lewis, L. B. Lunsford, R. Hromas, and C. T. Denny. The Ewing sarcoma EWS/FLI-1 fusion gene encodes a more potent transcriptional activator and is a more powerful transforming gene than FLI-1. *Mol. Cell. Biol.* **13**:7393–7398 (1993).
7. X. Mao, S. Miesfeldt, H. Yang, J. M. Leiden, and C. B. Thompson. The FLI-1 and chimeric EWS-FLI-1 oncoproteins

display similar DNA binding specificities. *J. Biol. Chem.* **269**:18216–18222 (1994).
8. W. A. May, M. L. Gishizky, S. L. Lessnick, L. B. Lunsford, B. C. Lewis, O. Delattre, J. Zucman, G. Thomas, and C. T. Denny. Ewing sarcoma 11;22 translocation produces a chimeric transcription factor that require the DNA-binding domain encoded by FLI1 for transformation. *Proc. Natl. Acad. Sci. USA* **90**:5752–5756 (1993).
9. K. Tanaka, T. Iwakuma, K. Harimaya, H. Sato, and Y. Iwamoto. EWS–Fli1 antisense oligodeoxynucleotide inhibits proliferation of human Ewing's sarcoma and primitive neuroectodermal tumor cells. *J. Clin. Invest.* **99**:239–247 (1997).
10. K. Hede. RNA-based nanoparticle treatment shows promise in Ewing's sarcoma model. *J. Natl. Cancer Inst.* **97**:627 (2005).
11. G. J. Hannon. RNA interference. *Nature* **418**:244–251 (2002).
12. A. Fire, S. Xu, M. K. Montgomery, S. A. Kostas, S. E. Driver, and C. C. Mello. Potent and specific genetic interference by double-stand RNA in *Caenorhabditis elegans*. *Nature* **391**: 806–811 (1998).
13. M. Pal-Bhadra, U. Bhadra, and J. A. Birchler. RNAi related mechanisms affect both transcriptional and posttranscriptional transgene silencing in *Drosophila*. *Mol. Cell* **9**:315–327 (2002).
14. S. M. Elbashir, J. Martinez, A. Patkaniowska, W. Lendeckel, and T. Tuschl. Functional anatomy of siRNAs for mediating efficient RNAi in *Drosophila melanogaster* embryo lysate. *EMBO J.* **20**:6877–6888 (2001).
15. E. Bernstei, A. A. Caudy, S. M. Hammond, and G. J. Hannon. Role for a bidentate ribonuclease in the initiation step of RNA interference. *Nature* **409**:363–366 (2001).
16. T. R. Brummelkamp, R. Bernards, and R. Agami. A system for stable expression of short interfering RNAs in mammalian cells. *Science* **296**:550–553 (2002).
17. T. R. Brummelkamp, R. Bernards, and R. Agami. A system for stable expression of short interfering RNAs in mammalian cells. *Science* **296**:550–553 (2002).
18. W. M. Bertling, M. Gareis, V. Paspaleeva, A. Zimmer, J. Kreuter, E. Nurnberg, and P. Harrer. Use of liposomes, viral capsids, and nanoparticles as DNA carriers. *Biotechnol. Appl. Biochem.* **13**:390–405 (1991).
19. Z. Hassani, G. F. Lemkine, P. Erbacher, K. Palmier, G. Alfama, and C. Giovannageli, *et al.* Lipid-mediated siRNA delivery dowregulates exogenous gene expression in the mouse brain at picomolar levels. *J. Gene Med.* **7**:198–207 (2004).
20. Y. Zhang, Y. F. Zhang, J. Bryant, A. Charles, R. J. Boado, and W. M. Pardridge. Intravenous RNA interference gene therapy targeting the human epidermal growth factor receptor prolongs survival in intracranial brain cancer. *Clin. Cancer Res.* **10**:3667–3677 (2004).
21. K. M. Ray and P. A. Whittaker. RNA interference: from gene silencing to gene-specific therapeutics. *Pharmacol. Ther.* **107**:222–239 (2005).
22. G. Lambert, E. Fattal, H. Pinto-Alphandary, A. Gulik, and P. Couvreur. Polyisobutylcyanoacrylate nanocapsules containing an aqueous core as a novel colloidal carrier for the delivery of oligonucleotides. *Pharm. Res.* **17**:707–714 (2000).
23. T. Tuschl. Expanding small RNA interference. *Nat. Biotechnol.* **20**:446–448 (2002).
24. I. Aynie, C. Vauthier, M. Foulquier, C. Malvy, E. Fattal, and P. Couvreur. Development of a quantitative polyacrylamide gel electrophoresis analysis using a multichannel radioactivity counter for the evaluation of oligonucleotide-bound drug carrier. *Anal. Biochem.* **240**:202–209 (1996).
25. G. Lambert, J. R. Bertrand, E. Fattal, S. Subra, H. Pinto-Alphandary, C. Malvy, C. Auclair, and P. Couvreur. EWS Fli-1 antisense nanocapsules inhibits Ewing sarcoma-related tumor in mice. *Biochem. Biophys. Res. Commun.* **279**:401–406 (2000).
26. S. Watnasirichaikul, N. M. Davies, T. Rades, and I. G. Tucker. Preparation of biodegradable insulin nanocapsules from biocompatible microemulsions. *Pharm. Res.* **17**:684–689 (2000).
27. P. Workman, *et al.* United Kingdom Co-ordinating Committee on Cancer Research (UKCCCR) Guidelines for the Welfare of animals in Experimental Neoplasia (Second Edition). *Br. J. Cancer* **77**:1–10 (1998).
28. T. Maniatis E. F. Fritsch and J. Sambrook. *Molecular Cloning. A Laboratory Manual*, Cold Spring Harbor Laboratory, Cold Spring Harbor, NY, 1982.
29. M. R. Schiffelers, A. Ansari, J. Xu, Q. Zhou, Q. Tang, G. Storm, G. Molema, P. Y. Lu, P. V. Scaria, and M. C. Woodle. Cancer siRNA therapy by tumor selective delivery with ligand-targeted sterically stabilized nanoparticle. *Nucleic Acids Res.* **32**:e149 (2004).
30. W. Zhang, H. Yang, X. Kong, S. Mohapatra, H. San Juan-Vergara, G. Hellermann, S. Behera, R. Singam, R. F. Lockey, and S. S. Mohapatra. Inhibition of respiratory syncytial virus infection with intranasal siRNA nanoparticles targeting the viral NS1 gene. *Nat. Med.* **11**:56–62 (2005).
31. L. Spahn, C. Siligan, R. Bachmaier, J. A. Schmid, D. N. Aryee, and H. Kovar. Homotypic and heterotypic interactions of EWS, Fli1 and their oncogenic fusion protein. *Oncogene* **9**(22): 6819–6829 (2003).
32. Y. L. Chiu, A. Ali, C. Y. Chu, H. Cao T. M. Rana. Visualizing a correlation between siRNA localization, cellular uptake, and RNAi in living cells. *Chem. Biol.* **11**:1165–1175 (2004).
33. Q. Leng and A. J. Mixson. Small interfering RNA targeting Raf-1 inhibits tumor growth *in vitro* and *in vivo*. *Cancer Gene Ther.* **12**(8): 682–690 (2005).
34. H. Guan, Z. Zhou, H. Wang, W. L. Jia, and W. L. Kleinerman. A small interfering RNA targeting vascular endothelial growth factor inhibits Ewing's sarcoma growth in a xenograft mouse model. *Clin. Cancer Res.* **11**:2662–2669 (2005).
35. A. Maksimenko, V. Polard, M. Villemeur, H. Elhamess, P. Couvreur, J. R. Bertrand, M. Aboubakar, M. Gottikh, and C. Malvy. *In vivo* potentialities of EWS-FLI-1 targeted antisense oligonucleotides–nanospheres complexes. *Ann. N.Y. Acad. Sci.* **1058**:52–62 (2005).
36. H. Farhood, N. Serbina, and L. Huang. The role of dioleoyl phosphatidylethanolamine in cationic liposome mediated gene transfer. *Biochim. Biophys. Acta* **1235**:289–295 (1995).